13th IEA Heat Pump Conference
April 26-29, 2021 Jeju, Korea

Empirical Analysis of Dehumidification Performance of Hollow-Fiber-Membrane Dehumidifier

Seong-Yong Cheon[a], Hye-Jin Cho[a], Jinyoung Ko[a], Jae-Weon Jeong[a,*]

[a]Department of Architectural Engineering, College of Engineering, Hanyang University,
222 Wangsimni-Ro, Seongdong-Gu, Seoul 04763, Republic of Korea

Abstract

Membrane dehumidifiers dry air via an isothermal process, which is why they can potentially yield a better dehumidification performance than conventional dehumidification systems. In this research, the dehumidification performance of a hollow-fiber-membrane dehumidifier was estimated by means of a series of experiments. The membrane dehumidifier consists of a hollow-fiber-membrane unit and an air pump. As the prototype unit used a sweep-gas, the use of dehumidified air was a drawback on the permeate side. Five operating parameters were considered as effective dehumidification variables: inlet air temperature, inlet air relative humidity, intake air flow rate, sweep gas ratio, and inlet air pressure. The dehumidification performance of the membrane dehumidifier was quantified as the difference in the humidity ratio and amount of dehumidification. The experimental data were analyzed by means of a parametric study involving the five independent operating parameters. Consequently, we found that the dehumidification performance was significantly impacted by the inlet air pressure that formed the driving force, and the inlet air conditions also exhibited a positive correlation with performance. When the sweep-gas ratio ranged from 0.4 to 0.6, a high value of dehumidification was achieved under balanced flow conditions.

Selection and/or peer-review under responsibility of the organizers of the 13th IEA Heat Pump Conference 2020.

Keywords: Membrane dehumidifier, Dehumidification performance, Empirical analysis;

1. Introduction

Desiccant-based air-conditioning technologies have recently been proposed for decoupling dehumidification and sensible cooling as an alternative to conventional cooling and dehumidification systems [1,2]. Desiccant-material-based systems pre-condition the intake outdoor air, and subsequently, the dehumidified air is controlled by a mechanical and evaporative cooling system to achieve the target temperature. Decoupled air-conditioning systems can afford high energy savings when the significant amount of heat consumed for regenerating the desiccant material is supplied by free energy [3–5].

Recently, membrane-based dehumidification systems have been suggested as an alternative system of vapor compression and desiccant-based dehumidification [6,7]. There is no requirement for a cooling and heating source as isothermal processes in such systems, compared with conventional dehumidification systems. In a membrane dehumidification system, the intake air is dehumidified via transferring water vapor between hydrophilic membrane layers by the application of a partial vapor gradient [6]. When a vapor pressure gradient is generated between membrane layers, the water vapor in the process air soaks and diffuses to the membrane layer, and subsequently, the layer is desorbed by another air stream. In this regard, several studies have investigated the dehumidification performance of membrane driers made of various materials under several design conditions [8,9]. Bui et al. [8] theoretically investigated a membrane dehumidification system with a flat plate. The membrane materials were assumed to consist of ceramic and polymeric layers with high

* Corresponding author. Tel.: +82-2-2220-2370; fax:+82-2-2220-1945.
E-mail address: jjwarc@hanyang.ac.kr (J.-W. Jeong).

permeability and selectivity of water vapor. The study results showed that the factors affecting the dehumidification performance included air velocity, permeability and selectivity of the membrane, pressure, and humidity of the processed air. Here, we note that membrane selectivity and pressure significantly affect a membrane drier's performance. Moreover, some studies have considered the use of membrane dehumidification systems for the air-conditioning of buildings; El-Dessouky et al. [10] proposed a membrane-dehumidifier-integrated air-cooling system, which has a vacuum-based membrane drier for dehumidification and evaporative coolers for sensible cooling. The authors showed that membrane-dehumidification-based air-conditioning systems can reduce the energy consumption by up to 86% when compared with conventional air-conditioning systems.

In this context, several studies have focused on membrane dehumidification systems to evaluate their energy and dehumidification performance for various membrane materials and system configurations. However, very few studies have experimentally evaluated the dehumidification performance of membrane dehumidification systems as applied to building heating, ventilation, and air-conditioning (HVAC). In this study, we developed a hollow-fiber-type membrane dehumidifier and evaluated its dehumidification performance under various operating conditions.

2. Hollow-fiber-membrane dehumidifier

In this section, we describe the general principle underlying membrane dehumidification along with the theoretical dehumidification process. Furthermore, we present our prototype hollow-fiber-membrane dehumidifier.

2.1 Hollow-fiber-membrane dehumidifier

The membrane dehumidifier dries the intake air via an isothermal process, which is hard to realize in conventional dehumidifiers. The membrane dehumidifier has two main parts: membrane modules and air compressor, as shown in Figure 1. The membrane module for dehumidification uses permeated water vapor, and the air compressor generates a partial vapor pressure gradient between the membrane layers. When the partial vapor pressure gradient between the membrane layers is created by the air compressor, the water vapor permeates from the feed side to the permeate side. The dehumidification performance is dependent on the membrane material, particularly its permeability and selectivity to water vapor. When the membrane affords a high level of permeability and selectivity, the dehumidification performance and energy efficiency of the membrane unit is correspondingly higher. In this study, the type of membrane used is a hollow-fiber membrane, which is easy to manufacture structurally, and the air compressor is used to pressurize the inlet air for creating the vapor pressure gradient between membrane layers. To maintain the dehumidification performance, a part of the intake air is "swept" out to the permeate side, thereby removing the water vapor.

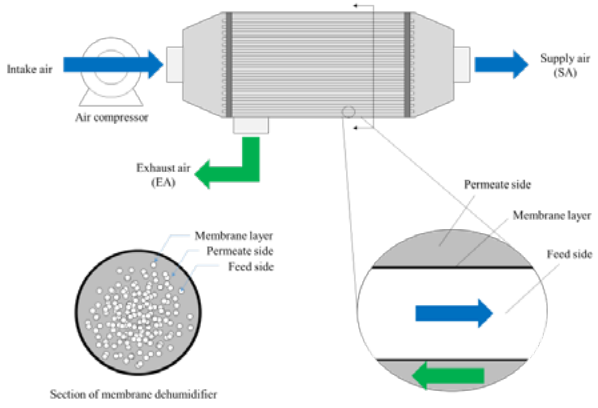

Fig. 1. Configuration of hollow-fiber-membrane dehumidifier

When the intake gas is assumed to be an ideal mixture of two gases, dry air and water vapor, the dehumidification process of the membrane dehumidifier can be represented by a solution–diffusion process between the feed side and the permeate side with a partial pressure gradient, as shown in Figure 2. When the feed-side air of the unit is pressurized for dehumidification, water vapor and dry air permeate through the membrane layer. The molar mass flow rates of water vapor and dry air (i.e., $\dot{M}'_w$ and $\dot{M}'_d$) through the membrane layer are estimated by means of the classical solution–diffusion model as represented by Equations (1) and (2), respectively. To estimate the partial pressure gradient, which acts as the force driving the dehumidification, we represent the partial pressure of each gas on the permeate side as the ratio of the molar mass flow rate through the membrane layer (i.e., y_1 and y_2) in Equations (3) and (4). The values of permeability (Per), selectivity (S), membrane area (A_{mem}), and membrane thickness (z) are determined according to the performance of the membrane materials, and these values affect the dehumidification performance along with energy consumption of the air compressor. Each molar mass flow rate is dependent on the membrane material and sweep gas used to remove the water vapor on the permeate side.

$$\dot{M}'_w = \frac{\mathrm{Per}_v A_{mem}}{z}\left(P_{f,v} - y_1 P_{p,tot}\right) \tag{1}$$

$$\dot{M}'_d = \frac{\mathrm{Per}_d A_{mem}}{z}\left(P_{f,d} - y_2 P_{p,tot}\right) = \frac{\mathrm{Per}_v}{S}\frac{A_{mem}}{z}\left(P_{f,v} - y_2 P_{p,tot}\right) \tag{2}$$

$$y_1 = \frac{\dot{M}'_v + \dot{M}'_{sweep,v}}{\dot{M}'_d + \dot{M}'_v + \dot{M}'_{sweep,d} + \dot{M}'_{sweep,v}} \tag{3}$$

$$y_2 = \frac{\dot{M}'_d + \dot{M}'_{sweep,d}}{\dot{M}'_d + \dot{M}'_v + \dot{M}'_{sweep,d} + \dot{M}'_{sweep,v}} \tag{4}$$

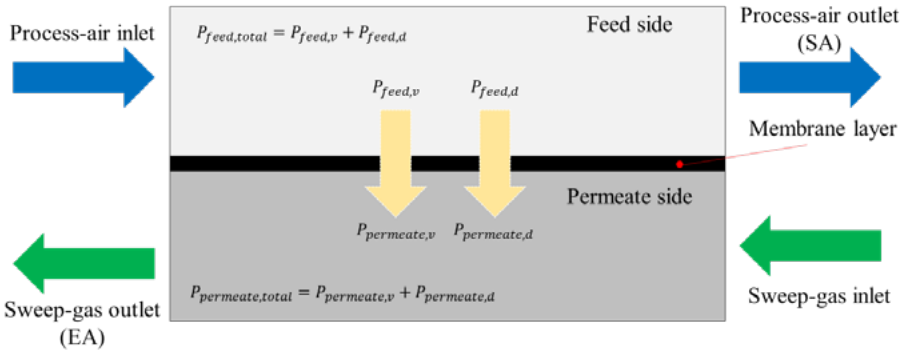

Fig. 2. Schematic of dehumidification process in membrane dehumidifier

2.2 Prototype of hollow-fiber-membrane dehumidifier

When the basic theoretical model does not consider the membrane type and configuration, it is not easy to estimate the dehumidification performance of the membrane dehumidifier under various operating conditions. Therefore, we developed a prototype hollow-fiber-membrane dehumidifier and estimated its dehumidification performance under various conditions. The configuration of the prototype unit is shown in Figure 3. The prototype unit has an inlet air channel on the feed side and sweep-gas air channel on the permeate side. In the study, the membrane module of our proposed dehumidifier was of the cylinder type, and the length of the module was 0.3 m, with the module diameter being 0.08 m. The module contained 170 hollow-fiber membranes each with a fiber inlet diameter of 1.6 mm, corresponding to a packing fraction ratio of 0.11. The hollow-fiber length was 0.23 m, and its total effective contacting area was 0.282 m^2. The specifications of our prototype module are listed in Table 1.

Table 1: Specifications of prototype unit

Design parameters	Values	Design parameters	Values
Module diameter [mm]	80	Fiber thickness [mm]	0.35
Module length [mm]	300	Contacting area of membrane [m^2]	0.282
Fiber inlet diameter [mm]	1.6	Number of fibers [-]	170
Fiber outlet diameter [mm]	2.3	Packing fraction [-]	0.11
Fiber length [mm]	230		

Fig. 3. Prototype configuration of hollow-fiber-membrane dehumidifier

3. Test setup and dehumidification performance

3.1 Experimental setup of prototype

To analyze the dehumidification performance of our prototype unit, we varied five independent parameters: air temperature, relative humidity, airflow rate, inlet air pressure, and sweep-gas ratio. The experimental setup for controlling these five independent parameters is shown in Figure 4. In the setup, the environmental chamber is used to maintain the experimental air conditions, and the air compressor maintains the airflow ratio of the conditioned air to the prototype unit. The rotation speed of the air compressor is controlled by means of a switched-mode power supply (SMPS) that controls the electric current and voltage. The pressure of the feed side is controlled by open-to-close ratio of the inlet valves to generate the partial pressure gradient. Moreover, the sweep-gas ratio, which corresponds to the ratio of the intake supply airflow rate to the sweep-gas flow rate, is controlled by the outlet valve as an adjustable open-to-close ratio. The measured data to estimate the dehumidification performance of the prototype unit are collected and saved in the data logger.

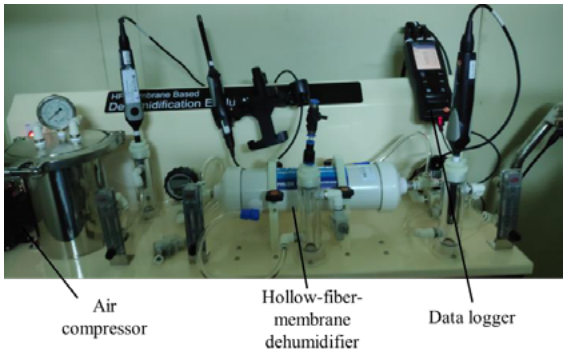

Fig. 4. Schematic of experimental setup of hollow-fiber-membrane dehumidifier

3.2 Operation conditions

In this study, we conducted 24 sets of experiments for analyzing the dehumidification performance of the hollow-fiber-membrane dehumidifier unit. The dehumidification performance of the prototype unit was estimated as the differential of the humidity ratio and amount of dehumidification, as expressed by Equations (5) and (6), respectively. The humidity ratio differential is representative of the driving force of the vapor pressure gradient, and the amount of dehumidification represents the dehumidification per unit time as a function of the latent cooling capacity.

$$\Delta w = w_{in} - w_{out} \quad (5)$$

$$\dot{m}_d = \dot{m}_{sa}\Delta w = (\dot{m}_{intake} - \dot{m}_{sweep})\Delta w \quad (6)$$

To analyze the dehumidification performance under various conditions, we acquired the performance data for various values of the five operating parameters: air temperature, relative humidity, airflow rate, sweep-gas ratio, and inlet air pressure. As the sweep-gas ratio is the airflow ratio of the intake air to the sweep-out air, a high level of sweep gas implies that the supply airflow rate is reduced for a given intake air flow rate. To estimate the differential of the humidity ratio and amount of dehumidification, each parameter was suitably varied. As the air temperature and humidity ratio were set to reflect humid and mild air conditions, these were maintained in the range of 15 to 30 ℃ and 40 to 80%, respectively. The detailed operational range is listed in Table 2. To estimate the dehumidification performance of the prototype unit, we did parametric study from the experimental results, which were based on the base case, and subsequently, only a single parameter was modulated in the operation range when all other parameters were fixed.

Table 2: Operating ranges of experimental conditions

Parameter	Symbol	Input values		
		Low	Base	High
Inlet air temperature [℃]	$T_{a,in}$	15	27	30
Inlet relative humidity [%]	$RH_{a,in}$	40	60	80
Inlet air flow rate [l/min]	$\dot{V}_{a,in}$	20	25	30
Sweep-gas ratio [−]	x	0.18	0.5	0.82
Inlet pressure [kPa]	p_{air}	101.3	101.3	260

The measurement sensors in our setup included high-precision humidity/temperature, differential pressure, and absolute pressure sensors. The high-precision humidity/temperature sensor measures the inlet and outlet temperatures and relative humidity. The airflow rate is measured by the differential pressure sensor in conjunction with a digital flow meter. The measurement points corresponding to airflow rate measurements include the inlet, outlet, and exhaust sides. The inlet air pressure is measured by the absolute pressure sensor, where the inlet air pressure is controlled by the air compressor by means of valves. To quantify the dehumidification performance, the measurement data were converted into the humidity ratio, which is affected by the air temperature, relative humidity, and pressure.

Table 3: Specifications of measuring instruments

Variable	Device	Characteristics		
Dry-bulb temperature and relative humidity of air	High-precision humidity/temperature probe	Range	Temperature	−20 ℃ to +55 ℃
			Relative humidity	0%–100%
		Accuracy	Temperature	±0.4 ℃
			Relative humidity	±2%RH
Air flow rate	Differential pressure sensor	Range	Pressure	0–1250 Pa
		Accuracy		±0.30%
Inlet air pressure	Absolute pressure sensor	Range	Pressure	0–1250 Pa
		Accuracy		±0.30%

4. Experimental results and discussion

We experimentally investigated the performance of the prototype unit considering the influences of the five air inlet parameters: inlet air temperature, relative humidity, air pressure, inlet air flow rate, and sweep-gas ratio. The influence of each of the five parameters considered was analyzed via the differential of the humidity ratio and amount of dehumidification; the results are shown in Figure 5.

We note from the figure that the air temperature and relative humidity exhibit a positive correlation with the differential of the humidity ratio and amount of dehumidification. We note that higher levels of inlet temperature and relative humidity correspond to a higher partial vapor gradient between the membrane layers. In addition, as the inlet air pressure increases, the partial vapor pressure gradient between membrane layer was increased , and the dehumidification performance improves. The sweep-gas ratio and intake airflow rate exhibit no positive correspondence with the dehumidification performance. When the sweep-gas ratio ranges from 0.4 to 0.6, the differential of the humidity ratio and the amount of dehumidification are maximal because the mass transfer between the feed and permeate sides increases as a balanced flow. When the intake air flow rate decreases, the face velocity on the feed side also decreases with increase in the contact time of the unit. The differential of the humidity ratio is strongly affected, but the amount of dehumidification is only relatively impacted by the airflow rate.

The main parameters that significantly affect the dehumidification performance of the prototype unit are the inlet air pressure and sweep-gas ratio. To increase the dehumidification performance, the inlet air pressure should be sufficiently high, and the sweep-gas ratio must be maintained around 0.5 for balanced flow. Here, we note that to control the outlet humidity ratio, a suitable rotation speed modulation strategy of the air compressor or sweep-gas ratio should be estimated.

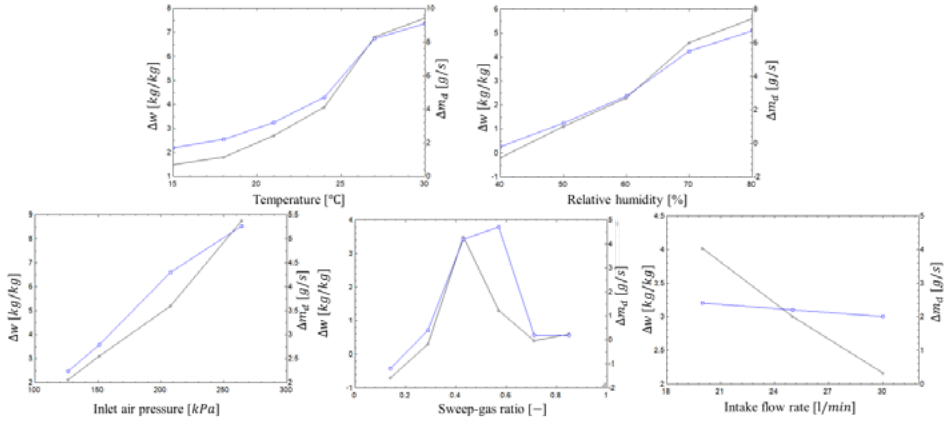

Fig. 5. Parametric analysis of hollow-fiber-membrane dehumidifier

5. Conclusions

In this study, we experimentally investigated the dehumidification performance of a hollow-fiber-membrane dehumidification unit. Our prototype unit was composed of a membrane module containing a bundle of hollow membranes and an air compressor to pressurize the inlet pressure, which forms the driving force underlying the process. Experiments were conducted using the prototype unit to estimate the differential of the humidity ratio and amount of dehumidification, and the relevant performance data were collected. The input parameters that influence the dehumidification performance are the air temperature, relative humidity, inlet air pressure, sweep-gas ratio, and intake air flow rate. The air temperature and relative humidity exhibited a positive correlation with the performance, which indicates that a larger amount of air with water vapor affords increased dehumidification performance. The inlet air pressure also positively affects the performance via increasing the driving force of the vapor pressure drop. The dehumidification performance was maximal when the sweep-gas ratio was in the range of 0.4 to 0.6 under balanced flow conditions. When the intake air flow rate was decreased, the dehumidification performance increased because of the increased contacting time of air with the prototype unit.

In future study, we plan to analyze the dehumidification efficiency under various operation conditions. In addition, the data collected in the study can be applied to extend the utilization of the control logic of the hollow-fiber-membrane dehumidifier.

Acknowledgements

This work was supported by the National Research Foundation of Korea (NRF) grant (No. 2019R1A2C2002514), the Korean Institute of Energy Technology Evaluation and Planning (KETEP) (No. 20184010201710), and the Technology development Program(S2782284) funded by the Ministry of SMEs and Startups(MSS, Korea).

References

[1] Rafique MM, Gandhidasan P, Bahaidarah HMS. Liquid desiccant materials and dehumidifiers - A review, *Renew. Sustain. Energy Rev* 2016;56:179–195.
[2] Ling J, Hwang Y, Radermacher R. Theoretical study on separate sensible and latent cooling air-conditioning system, *Int. J. Refrig* 2010;33:510–520.
[3] Yang Z, Lian Z, Li X, Zhang K. Concept of dehumidification perfectness and its potential applications, *Energy* 2015; 91:176–191.
[4] Gommed K, Grossman G. Experimental investigation of a liquid desiccant system for solar cooling and dehumidification, *Sol. Energy* 2007;81:131–138.
[5] Misha S, Mat S, Ruslan MH, Sopian K. Review of solid/liquid desiccant in the drying applications and its regeneration methods, *Renew. Sustain. Energy Rev* 2012;16:4686–4707.
[6] Woods J. Membrane processes for heating, ventilation, and air conditioning, *Renew. Sustain. Energy Rev* 2014;33:290–304.
[7] Labban O, Chen T, Ghoniem AF, Lienhard JH, Norford LK. Next-generation HVAC: Prospects for and limitations of desiccant and membrane-based dehumidification and cooling, *Appl. Energy* 2017;200:330–346.
[8] Bui DT, Nida A, Ng KC, Chua KJ. Water vapor permeation and dehumidification performance of poly(vinyl alcohol)/lithium chloride composite membranes, *J. Memb. Sci* 2016;498:254–262.
[9] Bui DT, Wong Y, Islam MR, Chua KJ. On the theoretical and experimental energy efficiency analyses of a vacuum-based dehumidification membrane, *J. Memb. Sci* 2017;539:76–87.
[10] El-Dessouky HT, Ettouney HM, Bouhamra W. A novel air conditioning system: membrane air drying and evaporative cooling, *Chem Eng Res Des* 2002;78:999–1009.